Density-matrix spectra for integrable models

Ingo Peschel* and Matthias Kaulke†
Fachbereich Physik, Freie Universität Berlin,
Arnimallee 14, D-14195 Berlin, Germany

Örs Legeza‡
Research Institute for Solid State Physics
P.O. Box 49, H-1525 Budapest, Hungary

February 1, 2008

Abstract

The spectra which occur in numerical density-matrix renormalization group (DMRG) calculations for quantum chains can be obtained analytically for integrable models via corner transfer matrices. This is shown in detail for the transverse Ising chain and the uniaxial *XXZ* Heisenberg model and explains in particular their exponential character in these cases.

Keywords: Density-matrix renormalization; Integrable systems; Corner transfer matrices

*email: peschel@physik.fu-berlin.de
†email: kaulke@physik.fu-berlin.de
‡email: olegeza@power.szfki.kfki.hu

1 Introduction

The density-matrix renormalization group (DMRG) introduced by White in 1992 [1] is a numerical procedure by which one-dimensional quantum systems can be treated with spectacular accuracy. It is not difficult to obtain the ground-state energy for spin chains with 100 sites up to nine decimal places [2]. Correlation functions can be calculated as well and the DMRG has therefore become an important new tool in this area of physics.

The basis of the method is a proper selection of states in the Hilbert space which are important for the target state one wants to study. This is done by dividing the system into two parts with corresponding reduced density matrices ϱ_1 and ϱ_2. The relevant states in each part are then given by those eigenvectors of the ϱ_α which have the largest eigenvalues. Thus the spectra of the ϱ_α enter in an essential way and it is obvious that the method will only work well if the eigenvalues drop rapidly enough so that a small number of states is sufficient and practically exhausts the sum rules $\mathrm{Tr}(\varrho_\alpha) = 1$. Spectra of such a form, where the eigenvalues decrease roughly exponentially, have indeed been observed in various calculations [1, 3]. Somewhat surprisingly, however, no detailed investigation or discussion of their origin has been given so far. In this article we want to present such a study for two particular systems, the Ising chain in a transverse field and the XXZ Heisenberg chain.

Although these systems are integrable and their ground states are known, a direct determination of the corresponding ϱ_α is difficult. Therefore, we first relate the quantum chains to two-dimensional classical systems, namely the Ising model and the six-vertex model. As pointed out by Nishino et al. [4], the density matrices ϱ_α then become partition functions of strips with a cut and these can, in turn, be expressed as products of corner transfer matrices (CTM's) à la Baxter [5]. This feature *per se* is quite general. For integrable models, however, the spectra of such CTM's are known in the thermodynamic limit and have, in fact, exponential form, i.e. $\omega_n \sim \exp(-\alpha\, n)$ with integer n. Provided the correlation length ξ of the system is much smaller than the strip width or chain length L, the same should then hold for the ϱ_α. This is, indeed, the case: The spectra obtained from DMRG calculations are found to agree very well with the CTM results, both in their exponential form and in the predicted degeneracies. Deviations occur only at the lower end where finite-size and geometry effects are visible. In this way one obtains a simple and consistent picture of the density-matrix spectrum and its origin.

In the following we first describe the relation between density matrix and CTM and recall the results available for the latter. Then we present the numerical calculations for the two chains and the comparison with the analytical predictions. The conclusion contains some further discussion, also with respect to non-integrable and to critical systems.

2 Density matrices and corner transfer matrices

Consider a spin one-half quantum chain with L sites and Hamiltonian H. The density matrix constructed from the ground state $|\Phi\rangle$ is

$$\varrho = |\Phi\rangle\langle\Phi| \tag{1}$$

or in a matrix notation, with $\boldsymbol{\sigma} = \{\sigma_1, \sigma_2, \ldots, \sigma_L\}$ denoting a spin configuration of the chain and assuming Φ to be real,

$$\varrho(\boldsymbol{\sigma}, \boldsymbol{\sigma}') = \Phi(\boldsymbol{\sigma})\Phi(\boldsymbol{\sigma}'). \tag{2}$$

By taking partial traces one obtains the reduced density matrices which are of interest in the following. Writing $\boldsymbol{\sigma}_1 = \{\sigma_1, \sigma_2, \ldots, \sigma_M\}$ and $\boldsymbol{\sigma}_2 = \{\sigma_{M+1}, \sigma_{M+2}, \ldots, \sigma_L\}$ one has

$$\varrho_1(\boldsymbol{\sigma}_1, \boldsymbol{\sigma}_1') = \sum_{\boldsymbol{\sigma}_2} \Phi(\boldsymbol{\sigma}_1, \boldsymbol{\sigma}_2)\Phi(\boldsymbol{\sigma}_1', \boldsymbol{\sigma}_2) \tag{3}$$

and similarly for ϱ_2.

Now imagine that there is a relation of the quantum chain to a two-dimensional lattice of classical spins. There are various possibilities for this. For example, H could be a derivative of the row-to-row transfer matrix T of the lattice, or T could arise from a Trotter decomposition of $\exp(-\beta H)$. Here we want to assume that the commutation relation

$$[H, T] = 0 \tag{4}$$

holds. Then the ground state $|\Phi\rangle$ of H is also an eigenstate of T, and if it also gives the maximal eigenvalue (which is the case in our examples), it can be obtained from an arbitrary starting vector by applying T a large number of times. Therefore $\Phi(\boldsymbol{\sigma})$ can be viewed as the partition function (properly normalized) of a half-infinite vertical strip with the spin configuration $\boldsymbol{\sigma}$ at the near end and an arbitrary one at the other, far away end. Similarly, $\varrho(\boldsymbol{\sigma}, \boldsymbol{\sigma}')$ can be regarded as the partition function for two such strips, one extending to $-\infty$ and the other one to $+\infty$, with end configurations $\boldsymbol{\sigma}$ and $\boldsymbol{\sigma}'$, respectively. The reduced density matrix ϱ_1, finally, is obtained by identifying $\boldsymbol{\sigma}_2$ and $\boldsymbol{\sigma}_2'$ and summing, i.e. by joining the two strips between sites $(M+1)$ and L, while the rest remains unconnected. Thus one arrives at the partition function of an infinite strip with a perpendicular cut in it.

This situation, first discussed in [6], is shown in Fig. 1. The strip in this case is formed by a diagonally oriented square lattice. The variables $\boldsymbol{\sigma}_1$ and $\boldsymbol{\sigma}_1'$ along the cut are shown as white circles, the $\boldsymbol{\sigma}_2$ as black ones. The dashed lines divide the system further and define four rectangular corner transfer matrices denoted by A, B, C and D. They are the partition functions of the corresponding lattice pieces and of Ramond type, i.e. without a common central spin [7]. It follows that

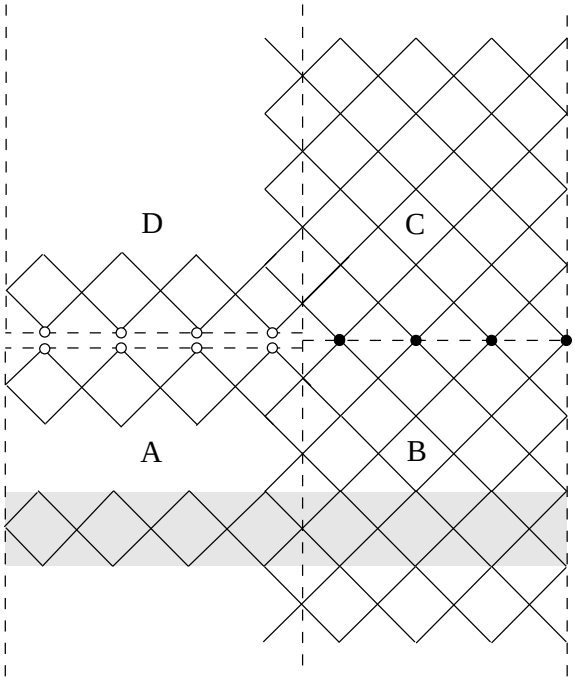

Figure 1: The strip geometry as discussed in the text with some portions of a square lattice. Also indicated are the corner transfer matrices A, B, C, D and the row transfer matrix (shaded).

$$\varrho_1 = ABCD. \tag{5}$$

This is the basic relation between the reduced density matrix and the CTM's [6, 8].

The CTM's which appear here differ somewhat from the usual ones. In calculations for finite-size systems one normally uses the shape shown in Fig. 2 [9, 10, 11, 12, 13]. The number of spins along both edges is then the same and one is dealing with square matrices. This is only a minor point, however, since also the products AB and CD in the strip are square matrices for $M = L/2$. The main point is that, for a large system away from criticality, the outer boundary plays a marginal role. In the CTM spectrum it affects only the lower end [10] and in the thermodynamic limit its effect vanishes so that one obtains a well-defined result.

For this reason the quantity

$$\hat{\varrho}_1 = \hat{A}\hat{B}\hat{C}\hat{D} \tag{6}$$

where the hat denotes the infinite-lattice limit will have the same spectrum as ϱ_1 corre-

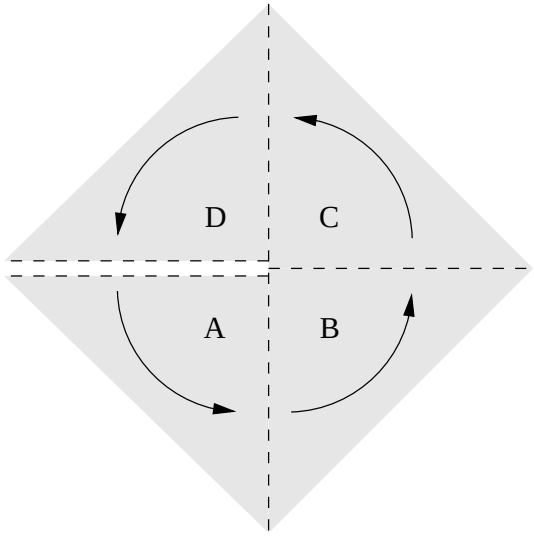

Figure 2: System composed of four corner transfer matrices with standard shape. The arrows indicate the direction of the transfer.

sponding to the strip, up to some deviations at the lower end and possibly some overall shift connected with the different normalizations of the quantities. For the infinite CTM's, however, the spectrum is known. Basically, it follows from the Yang-Baxter equations and the corner geometry [5]. The relevant results will be given in the next section.

3 Analytical results

For the treatment of the transverse Ising chain one considers the square lattice of Fig. 1 with Ising spins at the lattice points and an isotropic coupling K. The transfer matrix indicated by shading in the lower part of Fig. 1 commutes with the Hamiltonian [14, 15]

$$H = -\sum_{n=1}^{L-1} \sigma_n^x - \delta\sigma_L^x - \lambda \sum_{n=1}^{L-1} \sigma_n^z \sigma_{n+1}^z \tag{7}$$

where $\delta = \cosh 2K$ and $\lambda = \sinh^2 2K$. The enhancement of the transverse field at the right end can be neglected for large L. Then one arrives at the usual homogeneous chain.

The CTM's for this Ising lattice were studied in [16] and are exponentials of an operator which has again transverse Ising form but with site-dependent coefficients which increase

linearly with n. Due to the isotropy of the lattice all four matrices are equal and one has

$$\hat{\varrho}_1 = \hat{A}^4 = e^{-\hat{H}_{\rm CTM}} \tag{8}$$

where

$$\hat{H}_{\rm CTM} = c \left\{ \sum_{n\geq 1} (2n-1)\, \sigma_n^x + \lambda \sum_{n\geq 1} 2n\, \sigma_n^z \sigma_{n+1}^z \right\} \tag{9}$$

with a constant c depending on λ. The diagonalization of $\hat{H}_{\rm CTM}$ in terms of fermions [16, 11] then leads to

$$\hat{H}_{\rm CTM} = \sum_{j=0}^{\infty} \varepsilon_j n_j \tag{10}$$

with $n_j = c_j^\dagger c_j = 0, 1$ and the single-particle energies

$$\varepsilon_j = \begin{cases} (2j+1)\varepsilon & : \quad \lambda < 1 \quad (T > T_{\rm c}) & (11) \\ 2j\varepsilon & : \quad \lambda > 1 \quad (T < T_{\rm c}) & (12) \end{cases}$$

where ε is given by

$$\varepsilon = \pi \frac{I(k')}{I(k)}. \tag{13}$$

Here $I(k)$ denotes the complete elliptic integral of the first kind, $k' = \sqrt{1-k^2}$ and the parameter k with $0 \leq k \leq 1$ is related to λ by

$$k = \begin{cases} \lambda & : \quad \lambda < 1 & (14) \\ 1/\lambda & : \quad \lambda > 1. & (15) \end{cases}$$

An additive constant has been omitted in (10). From this one finds the following eigenvalues E for $\hat{H}_{\rm CTM}$.

(a). $\lambda < 1$

The ground state has $E = 0$. Excited states with one fermion lead to the odd levels $E = \varepsilon, 3\varepsilon, 5\varepsilon, \ldots$ With two fermions one obtains in addition all even levels *except* 2ε. The level 8ε is two-fold degenerate. The three-fermion excitations start at 9ε and lead to further degeneracies etc. The spacing of the E's, except at 2ε, is therefore ε.

(b). $\lambda > 1$

The ground state has again $E = 0$, but it is now twice degenerate due to the long range order. This leads to a corresponding two-fold degeneracy of all excited levels.

Formally, this follows from the fact that $\varepsilon_0 = 0$ [1]. The excited states are integer multiples of 2ε, i.e. the spacing of the E's is 2ε.

This is the well-known equidistant spectrum of $\hat{H}_{\rm CTM}$ with a spacing which depends on λ, i.e. on the distance from the critical point. It follows that up to degeneracies, which will be discussed later, $\hat{\varrho}_1$ has a purely exponential spectrum.

For the Heisenberg model, the associated two-dimensional system is the six-vertex model which is specified by three Boltzmann weights a, b, c [5]. If the vertex lattice is oriented parallel to the strip, its row-to-row transfer matrix commutes with the Hamiltonian [17]

$$H = \sum_n H_n \tag{16}$$

$$H_n = \sigma_n^x \sigma_{n+1}^x + \sigma_n^y \sigma_{n+1}^y + \Delta \sigma_n^z \sigma_{n+1}^z \tag{17}$$

where Δ is related to the vertex weights via $\Delta = (a^2+b^2-c^2)/(2ab)$. Strictly speaking, this holds only for periodic boundary conditions on T and H. As before, however, the effect of the boundaries should not matter for a large system. The non-critical case corresponds to $\Delta > 1$, so that H describes a uniaxial antiferromagnet.

The infinite CTM's for the six-vertex model are also known [5, 18, 19]. They are again exponentials of an operator similar to (16) but with site-dependent coefficients. Thus $\hat{\varrho}_1$ takes the form (8) and

$$\hat{H}_{\rm CTM} = c \sum_{n \geq 1} n H_n \tag{18}$$

where the constant c depends on Δ. Although the problem does not look like a free-fermion one, the eigenvalues of $\hat{H}_{\rm CTM}$ follow once more from (10) and (12), with ε now given by

$$\varepsilon = \operatorname{arcosh} \Delta. \tag{19}$$

Therefore the discussion for case (b) above can be taken over and one finds again an exponential spectrum for $\hat{\varrho}_1$.

4 Numerical calculations

In order to check these predictions we have carried out standard DMRG calculations for chains with up to 100 sites, keeping between 30 and 64 states in each block. The systems were built up via the infinite-size algorithm and ϱ_1 refers to one half of the chain. In the following, the eigenvalues ω_n of ϱ_1, ordered according to magnitude, are shown in

[1] The normalization of this state is discussed in [16].

semilogarithmic plots $\log \omega_n$ vs. n. All cases correspond to correlation lengths which do not exceed ten lattice spacings and thus are much smaller than L.

We begin with results for the transverse Ising chain. Fig. 3 shows an example of the spectrum in the disordered region ($\lambda < 1$). One can see that the first seven levels

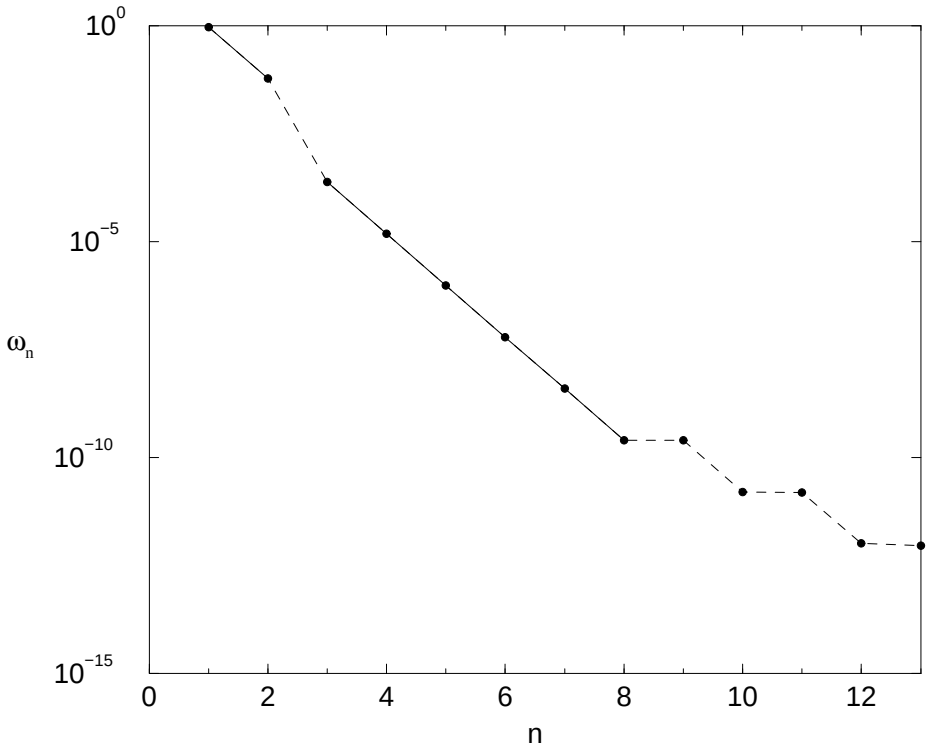

Figure 3: Density-matrix spectrum of a transverse Ising chain with $\lambda = 0.8$ and 120 sites, calculated with 30 states.

are non-degenerate and equidistant apart from a break between the second and the third one. This is exactly the pattern found for the E's of the infinite lattice in Section 3, case (a). The straight line through six of the levels shows clearly the linear behaviour and the level spacing (the slope in a plot $\ln \omega_n$ vs. n) agrees up to 10^{-3} with the theoretical value 2.7565 from (13). At the lower end, two-fold degeneracies are visible. Beyond that the spectrum becomes flat and no further structure can be seen. There, however, one is already at 10^{-14} and near the limits of the accuracy of the calculation. For larger values of λ, where the slope becomes smaller, the situation is more favorable.

The situation in the ordered phase is shown in Fig. 4 for $\lambda = 1.25$. One can see a

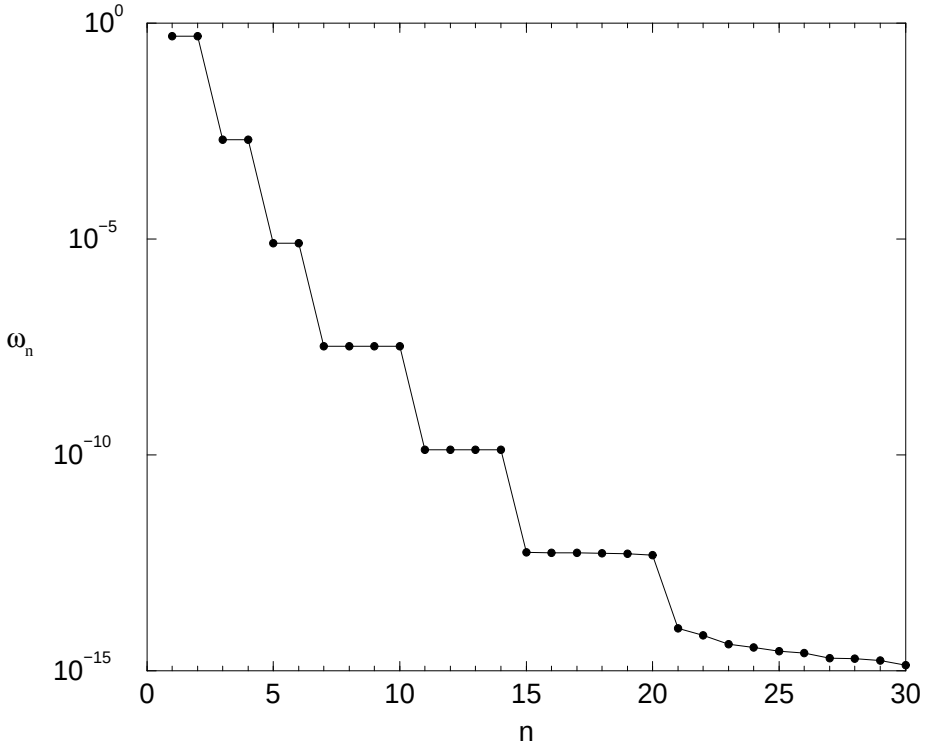

Figure 4: Density-matrix spectrum of a transverse Ising chain with $\lambda = 1.25$ and 120 sites, calculated with 30 states.

clear difference in the structure of the spectrum: There is no break and the multiplicities have changed. Their values (2,2,2,4,4,6,...) are just twice the number P_j of partitions of the integers $j = 0, 1, 2, \ldots$ and thus correspond exactly to what one expects according to Section 3 (b). Only the last multiplet is not correct. We attribute this to numerical inaccuracies.

The two-fold degeneracy needs some comments, though. In some calculations for longer chains it was lost and one observed two sets of levels (with degeneracies P_j) shifted with respect to each other. This can be traced back to a mixing of the ground state and the exponentially close first excited state of H in the numerical procedure, since at the same time the expectation value $\langle \sigma_n^z \rangle$ became non-zero. The mechanism can be discussed easily in the limit $\lambda \gg 1$, where

$$|\Phi\rangle \simeq \frac{1}{\sqrt{2}}\Big[|\Phi_+\rangle + |\Phi_-\rangle\Big] \tag{20}$$

with $|\Phi_+\rangle = |\uparrow\uparrow\cdots\uparrow\rangle$ and $|\Phi_-\rangle = |\downarrow\downarrow\cdots\downarrow\rangle$ being the two ferromagnetic states. This leads to

$$\varrho_1 \simeq \frac{1}{2}\Big[|\varphi_+\rangle\langle\varphi_+| + |\varphi_-\rangle\langle\varphi_-|\Big] \tag{21}$$

where the states $|\varphi_\pm\rangle$ now refer to part 1 of the chain. Thus ϱ_1 has two degenerate eigenvalues 1/2, the rest being zero. The same holds for the density matrix constructed from the first excited state

$$|\Phi'\rangle \simeq \frac{1}{\sqrt{2}}\Big[|\Phi_+\rangle - |\Phi_-\rangle\Big]. \tag{22}$$

However, a linear combination $a|\Phi\rangle + b|\Phi'\rangle$ with $a^2+b^2=1$ leads to eigenvalues $(a+b)^2/2$ and $(a-b)^2/2$, i.e. to a splitting. By targeting $|\Phi\rangle$ and $|\Phi'\rangle$ in a DMRG calculation and forming such linear combinations one can actually shift the two level sequences deliberately.

In Fig. 5 the pure spectra without the degeneracies are shown for several λ-values. One sees that the slope becomes smaller near the critical point ($\lambda = 1$), as it should, and a comparison of the numbers shows again very good agreement with the value 2ε for the spacing according to Section 3. Closer to the critical point, however, a larger number of states had to be kept. Also here the spectrum becomes flat around 10^{-14}.

For the *XXZ* chain, where only the ordered region and the critical phase exist, the situation is even better. Here one can work in the subspace $S^z = 0$ which makes the calculation more precise with the same number of kept states. Fig. 6 shows the complete spectrum for three values of the anisotropy Δ. In all cases, the first 10 levels can be observed and the degeneracies $2 \cdot (1, 1, 1, 2, 2, 3, 4, 5, 6, 8)$ can be read off clearly, even though some very low levels do not fit perfectly. In comparison to Fig. 4 the accuracy is much better here so that even at 10^{-18} the structures can be seen. This is a very convincing demonstration of the theoretically predicted scheme. The perfect two-fold degeneracy indicates that there is no admixture of the excited state here. This is in line with the observation that $\langle\sigma_n^z\rangle = 0$ in these calculations. Finally, in Fig. 7 pure spectra are shown together with linear fits for the first 8 levels. One should note that there is an arbitrariness in the definition of degeneracy. Here the criterion was a relative difference of less than 10^{-4}. If one relaxes this, the linear region becomes even larger. The ε-values given in the Figure agree with (19) up to 3-4 decimal places. Also here there is a flattening of the spectrum at the lower end. This, incidentally is in contrast to results for usual finite-size CTM's, where the spectrum becomes steeper at the lower end [10, 11, 13], and can have two origins: The different geometries of the systems in the two calculations (Figs. 1 and 2) and limitations due to the truncation in the DMRG procedure.

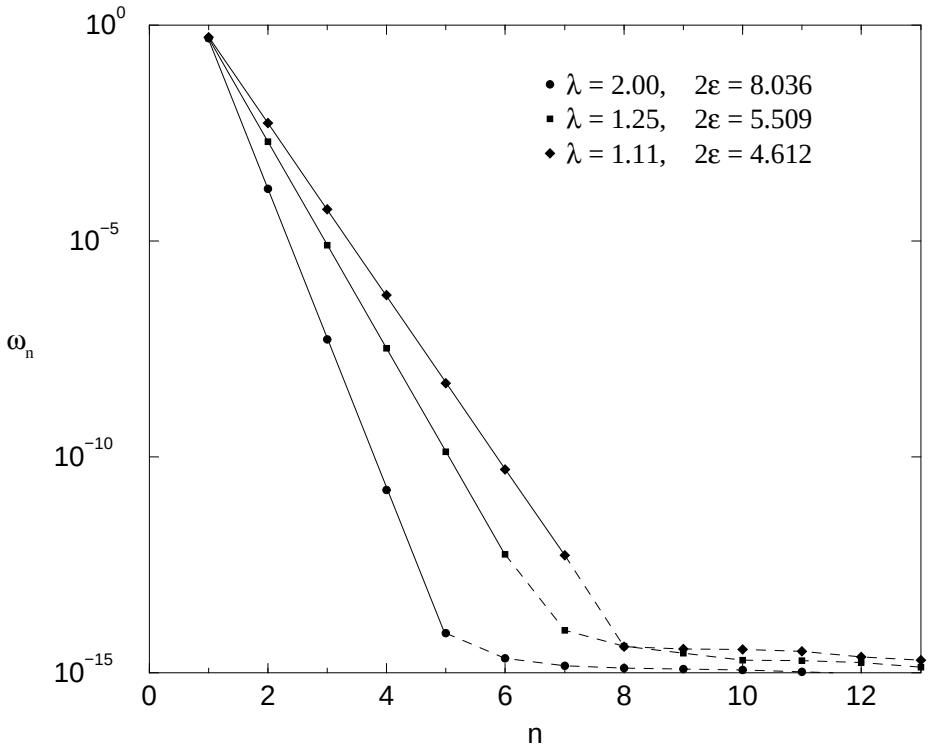

Figure 5: Density-matrix spectra of transverse Ising chains for three values of λ without the degeneracies, calculated with 30 states for $\lambda = 2$ and 1.25 and with 60 states for $\lambda = 1.11$. The ε-values were obtained from the slopes.

5 Conclusion

We have shown for two integrable, non-critical spin chains how the density matrix reflects the properties of the associated corner transfer matrices. The exponential character of its spectrum can in these cases be understood as a consequence of the star-triangle or Yang-Baxter equations.[2] The same will hold for other integrable models and one thereby obtains a whole class of examples, where the density-matrix spectrum can be obtained analytically. In such cases one could estimate in advance, how many states one has to keep in a DMRG calculation to get a certain accuracy. Since even for soluble models the correlation functions might have to be calculated numerically, this could be useful in

[2]It is amusing to note that such an exponential form arises also for two coupled harmonic oscillators [20].

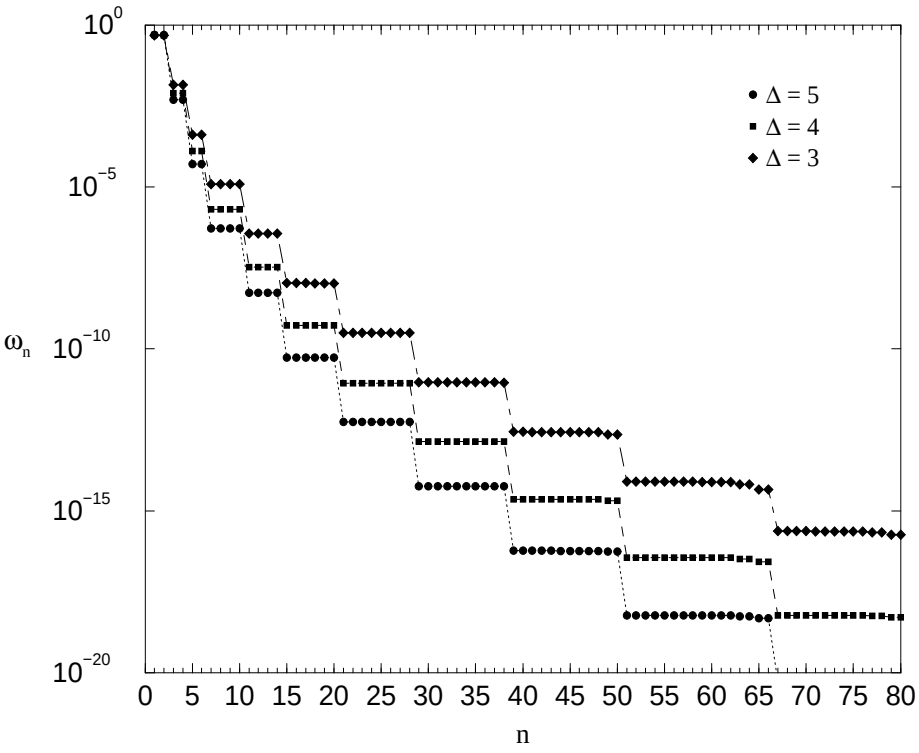

Figure 6: Density-matrix spectra of Heisenberg chains with 98 sites, calculated with 64 states for three values of Δ.

practice.

One immediate question concerns, of course, non-integrable systems. The connection to CTM's still exists, but there are no general results for their spectra. For the three-state Potts model, it was shown that the equidistance of the levels of H_{CTM} is lost for finite temperatures [21]. This is consistent with calculations of the ϱ_1-spectrum, which also show irregular level spacing, although the overall behaviour is still roughly exponential [22]. A recent investigation of other non-integrable models even indicates a kind of universality for the spectra [23]. The fact that the basic features of the CTM's are still similar was also used in direct renormalization calculations for these quantities [8].

The second question relates to critical systems. Actually a number of the chains treated by DMRG belong to this category. Therefore an understanding of the spectra for this case would be quite useful. One does not need integrability here, instead conformal invariance may be invoked. However, due to the infinite correlation length the shape of

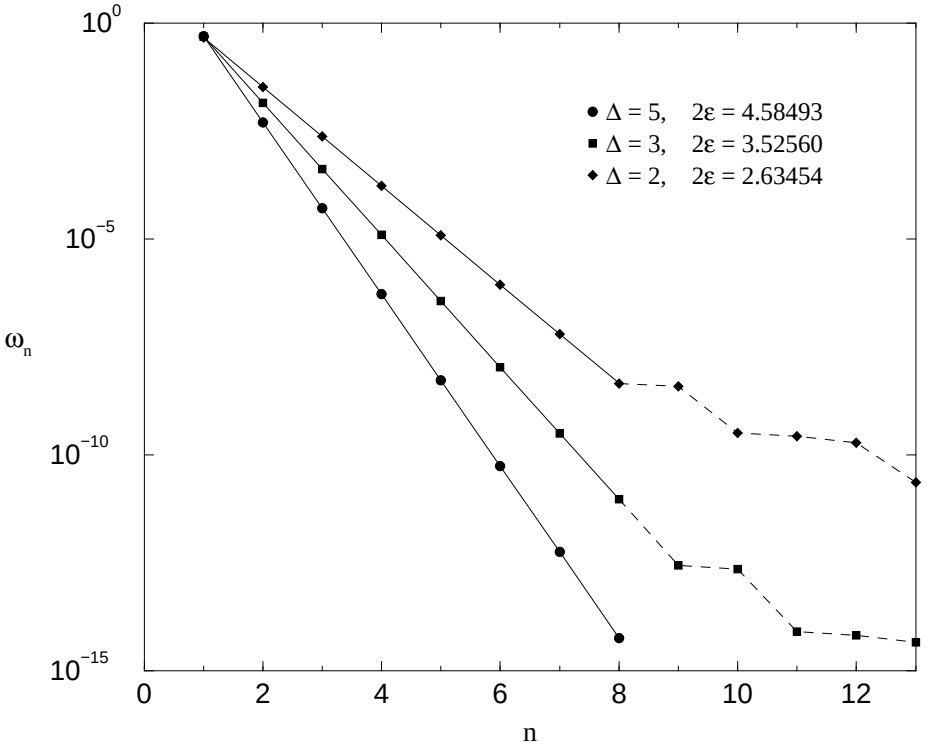

Figure 7: Density-matrix spectra of XXZ chains of 98 sites without the degeneracies, calculated with 64 states. The ε-values were obtained from the slopes.

the associated two-dimensional system is more important in this case. The CTM spectra have been investigated for the usual CTM geometry as in Fig. 2 [11, 12, 13] but one needs very large systems in order to see the linear spectrum of H_{CTM} and the logarithmic size dependence $\varepsilon \sim 1/\ln L$ predicted by conformal invariance. The same seems to hold for the strip geometry. This problem is presently still under investigation.

Acknowledgements

We thank D. Karevski for helpful contributions, T. Nishino and R. Noack for various discussions and C. Ritter for making his Potts results available. We also thank the Max-Planck-Institut für Physik komplexer Systeme in Dresden for its hospitality.

References

[1] S.R. White, Phys. Rev. Lett. **69** (1992) 2863; S.R. White, Phys. Rev. B **48** (1993) 10345

[2] Ö. Legeza, G. Fáth, Phys. Rev. B **53** (1996) 14349

[3] M. Kaulke, I. Peschel, Eur. Phys. J. B **5** (1998) 727

[4] T. Nishino, J. Phys. Soc. Japan **64** (1995) 3598

[5] R.J. Baxter, Exactly Solved Models in Statistical Mechanics, Academic Press, London 1982

[6] T. Nishino, K. Okunishi, Density Matrix and Renormalization for Classical Lattice Models, in: Srongly Correlated Magnetic and Superconducting Systems, ed. G. Sierra, M.A. Martín-Delgado, Lecture Notes in Physics Vol. 478, Springer, Berlin, Heidelberg, 1997 p. 167 (see also cond-mat/9610107)

[7] O. Foda, M. Jimbo, T. Miwa, K. Miki, A. Nakayashiki, J. Math. Phys. **35** (1994) 13

[8] T. Nishino, K. Okunishi, J. Phys. Soc. Japan **66** (1997) 3040

[9] R.J. Baxter, J. Stat. Phys. **15** (1976) 485; **17** (1977) 1

[10] T.T. Truong, I. Peschel, Z. Phys. B **69** (1987) 385

[11] T.T. Truong, I. Peschel, Z. Phys. B **75** (1989) 119

[12] I. Peschel, T.T. Truong, Ann. Physik **48** (1991) 185

[13] B. Davies, P.A. Pearce, J. Phys. A: Math. Gen. **23** (1990) 1295

[14] I. Peschel, Phys. Lett A **110** (1985) 313

[15] F. Iglói, P. Lajkó, J. Phys. A: Math. Gen. **29** (1996) 4803

[16] B. Davies, Physica A **154** (1988) 1

[17] B. Sutherland, J. Math. Phys. **11** (1970) 3183

[18] B. Davies, Physica A **159** (1989) 171

[19] B. Davies, Inifinite-dimensional symmetry of corner transfer matrices, in: Confronting the Infinite, ed. A.L. Carey et al., World Scientific, Singapore 1995 p. 193

[20] D. Han, Y.S. Kim, M.E. Noz, cond-mat/9705029 (1997)

[21] R. Wunderling, Diplomarbeit, Freie Universität Berlin 1991

[22] C. Ritter, Private communication

[23] K. Okunishi, Y. Hieida, Y. Akutsu, cond-mat/9810239 (1998)